frontiers | Frontiers in Oncology

TYPE Correction
PUBLISHED 11 October 2024
DOI 10.3389/fonc.2024.1495349

OPEN ACCESS

EDITED AND REVIEWED BY
João Pessoa,
University of Aveiro, Portugal

*CORRESPONDENCE
Mei Wang
wangmei8417@163.com
Feng Huang
huangfengksrmyy@163.com

RECEIVED 12 September 2024
ACCEPTED 17 September 2024
PUBLISHED 11 October 2024

CITATION
Wang M, Yu W, Cao X, Gu H, Huang J, Wu C, Wang L, Sha X, Shen B, Wang T, Yao Y, Zhu W and Huang F (2024) Corrigendum: Exosomal CD44 transmits lymph node metastatic capacity between gastric cancer cells via YAP-CPT1A-mediated FAO reprogramming. *Front. Oncol.* 14:1495349. doi: 10.3389/fonc.2024.1495349

Corrigendum: Exosomal CD44 transmits lymph node metastatic capacity between gastric cancer cells via YAP-CPT1A-mediated FAO reprogramming

Mei Wang [1]*, Wanjun Yu [1], Xiaoli Cao [2], Hongbing Gu [3], Jiaying Huang [1], Chen Wu [1], Lin Wang [1], Xin Sha [4], Bo Shen [5], Ting Wang [1], Yongliang Yao [6], Wei Zhu [1] and Feng Huang [1,6,7]*

[1]Key Laboratory of Medical Science and Laboratory Medicine of Jiangsu Province, School of Medicine, Jiangsu University, Zhenjiang, China, [2]Department of Laboratory Medicine, Affiliated Tumor Hospital of Nantong University, Nantong, China, [3]Department of Laboratory Medicine, The Affiliated People's Hospital, Jiangsu University, Zhenjiang, China, [4]Department of Surgery, The Affiliated Hospital of Jiangsu University, Jiangsu University, Zhenjiang, China, [5]Department of Oncology, Jiangsu Cancer Hospital, Jiangsu Institute of Cancer Research, Nanjing Medical University Affiliated Cancer Hospital, Nanjing, China, [6]Department of Clinical Laboratory, Affiliated Kunshan Hospital of Jiangsu University, Suzhou, China, [7]Department of Clinical Laboratory, Maternal and Child Health Care Hospital of Kunshan, Suzhou, China

KEYWORDS

exosomes, lymph node metastasis, gastric cancer, CD44, fatty acid oxidation, yes-associated protein (YAP), carnitine palmitoyltransferase 1A (CPT1A)

A Corrigendum on

Exosomal CD44 transmits lymph node metastatic capacity between gastric cancer cells via YAP-CPT1A-mediated FAO reprogramming

By Wang M, Yu W, Cao X, Gu H, Huang J, Wu C, Wang L, Sha X, Shen B, Wang T, Yao Y, Zhu W and Huang F (2022). *Front. Oncol.* 12:860175. doi: 10.3389/fonc.2022.860175

In the published article, there were errors in **Figure 1E**, **Figure 3C** and **Figures 4L–M** as published. Due to carelessness during the creation of the figures, images were pasted incorrectly. We found that **Figures 1E** (invasion, HGC-27) and 4L (migration, HGC-27-L ex si-CD44) do not correspond to the original data. Besides, the cell counts in **Figure 4M** do not match the observations in **Figure 4L**. For **Figure 3C**, the original data were lost, so independent repeat experiments were conducted, and the results were consistent with the initial findings. Thus, **Figures 3C, D** were updated.

The corrected **Figure 1** and its caption appear below.

The corrected **Figure 3** and its caption appear below.

The corrected **Figure 4** and its caption appear below.

The authors apologize for these errors and state that this does not change the scientific conclusions of the article in any way. The original article has been updated.

Publisher's note

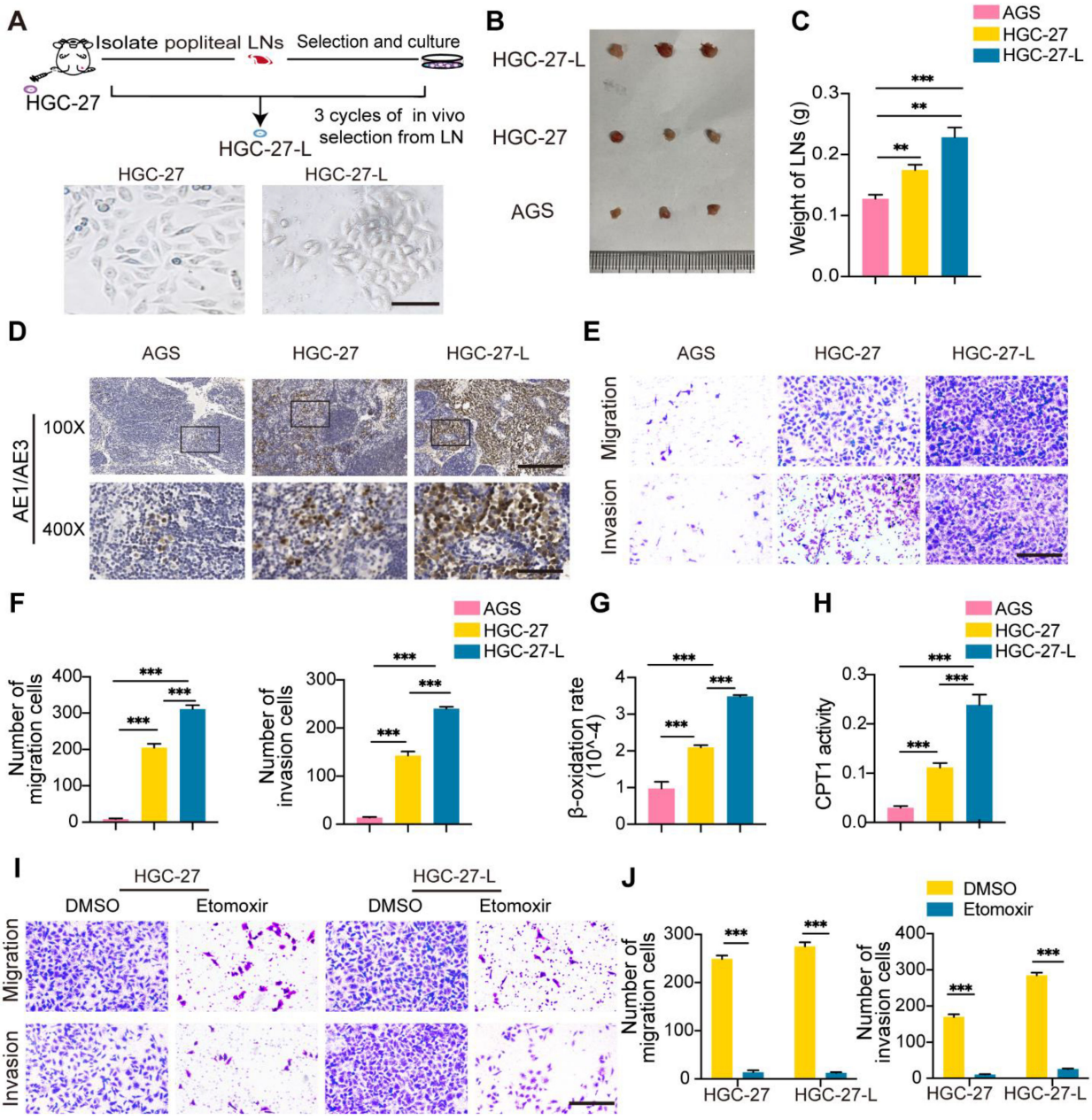

FIGURE 1
Establishment of a highly lymphatic metastatic GC cell line HGC-27-L and lymphatic metastatic GC cells sustained LNM capacity depending on FAO **(A)** A flow chart illustrates the establishment of HGC-27-L by serial transplantation of parental cell HGC-27 in vivo. Images of cell morphology are presented. (magnification, 400×; scale bars, 50 μm); (B–D) In vivo comparison of LNM capacity among AGS, HGC-27 and HGC-27-L by popliteal LNs analysis. **(B)** Pictures of LNs. Ruler unit, mm; **(C)** Weight of LNs; **(D)** Pancytokeratin AE1/AE3 staining (magnification, 100×; scale bars, 200 μm; magnification, 400×; scale bars, 50 μm); **(E, F)** In vitro comparison of migration and invasion capacity among the three cell lines. **(E)** Morphology of migrated and invaded cells (magnification, 200×; scale bars, 100 μm); **(F)** Count of migrated and invaded cells; **(G)** β-oxidation rate detection; **(H)** CPT1 activity analysis; **(I, J)** Effect of etomoxir treatment on migration and invasion capacity of HGC-27 and HGC-27-L cells. **(I)** Morphology of migrated and invaded cells (magnification, 200×; scale bars, 100 μm); **(J)** Number of migrated and invaded cells. $^{**}P < 0.01$; $^{***}P < 0.001$.

10.3389/fonc.2024.1495349

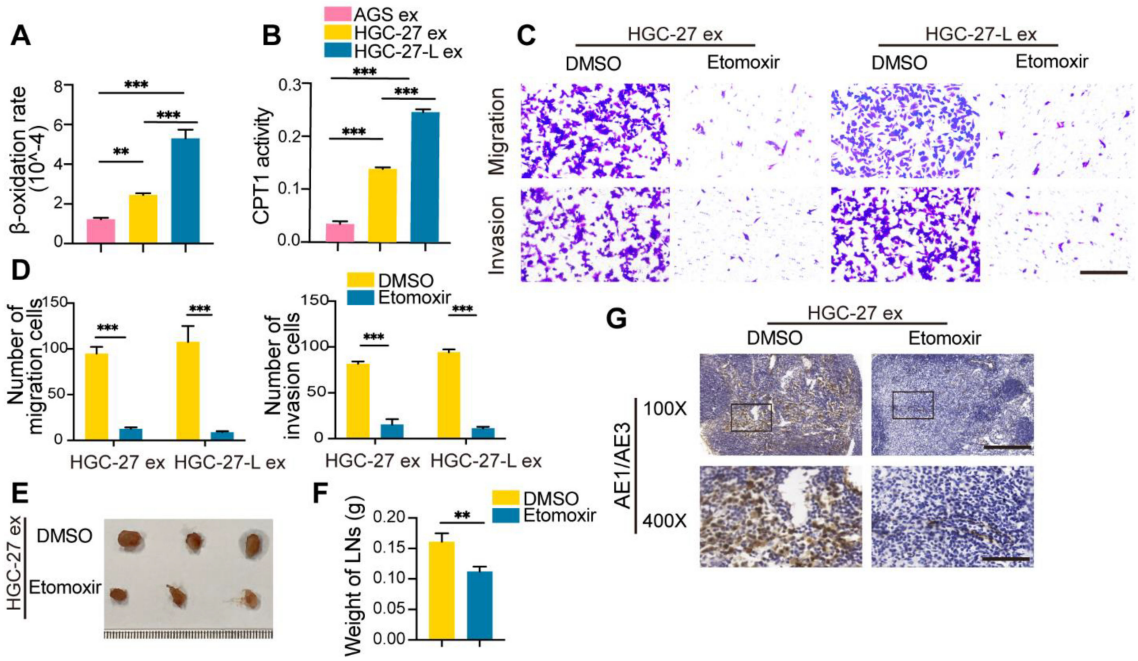

FIGURE 3
Lymphatic metastatic GC cell-exosomes conferred LNM capacity on primary GC cells depending on FAO **(A, B)** FAO detection in AGS after treatment with different GC cell exosomes. **(A)** β-oxidation rate measurement; **(B)** CPT1 activity analysis; **(C–G)** Effect of etomoxir pretreatment on lymphatic metastatic GC cell-exosome increasing AGS LNM capacity. **(C, D)** In vitro migration and invasion assay. **(C)** Representative images of migrated and invaded cells (magnification, 200×; scale bars, 100 μm); **(D)** Number of migrated and invaded cells; **(E–G)** In vivo LNM capacity detection. **(E)** Images of popliteal LNs. Ruler unit, mm; **(F)** Weight of LNs; **(G)** Pancytokeratin AE1/AE3 staining in LNs (magnification, 100×; scale bars, 200 μm; magnification, 400×; scale bars, 50 μm); ex, exosomes. $^{**}P < 0.01$; $^{***}P < 0.001$.

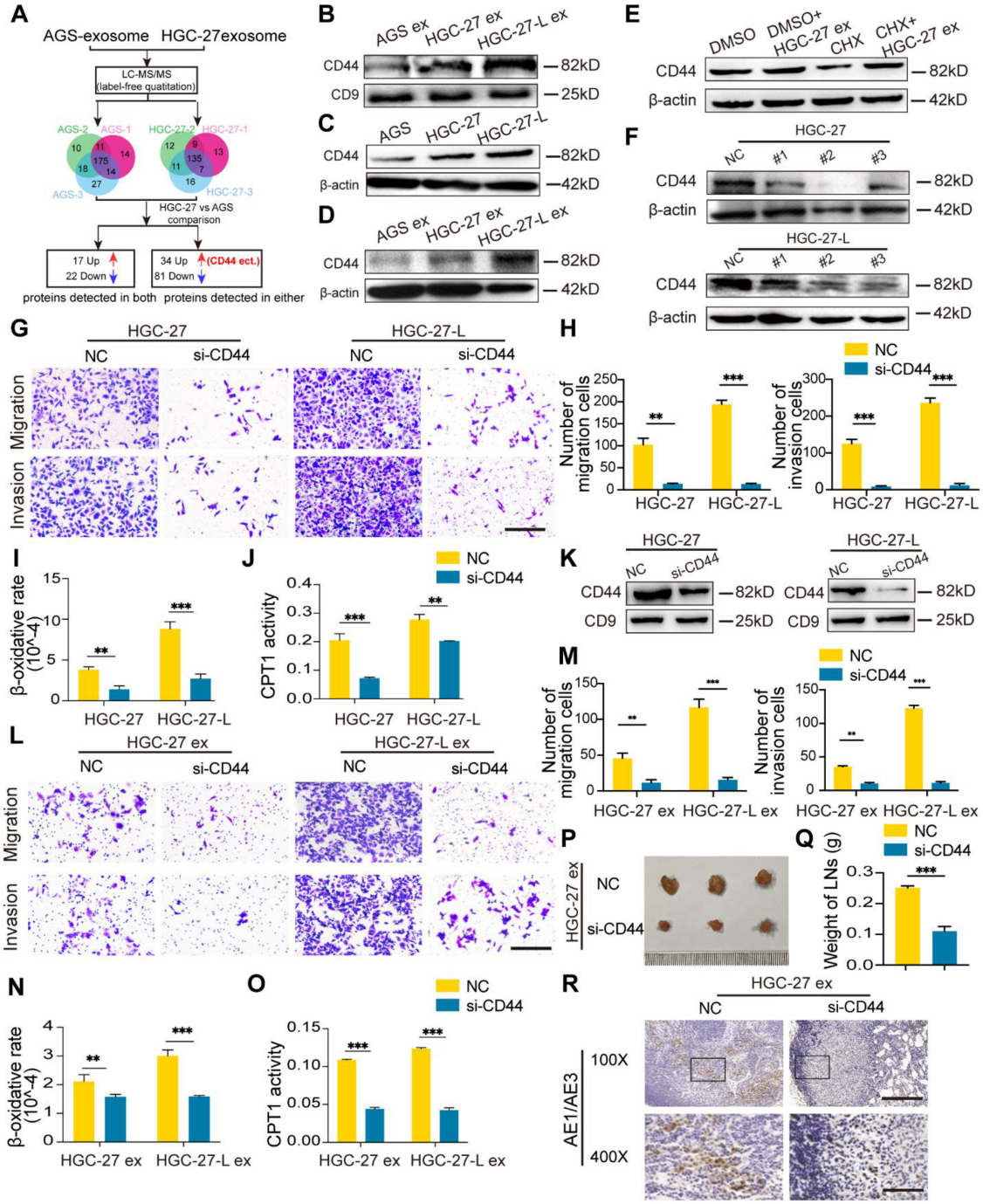

FIGURE 4
Identification of CD44 was a critical protein mediating exosome- transmission of LNM phenotype **(A)** A flow chart shows the identification of differential protein profile between HGC-27-exosomes and AGS-exosomes by label-free quantitation; **(B)** CD44 protein detection in different GC cell-exosomes; **(C)** Comparison of CD44 protein in GC cells; **(D)** Change of CD44 protein levels in AGS after treatment with exosomes; **(E)** Effect of CHX pretreatment on CD44 protein in AGS incubation with HGC-27-exosomes; **(F)** Screening for the most efficient si-CD44 in HGC-27 and HGC-27-L; **(G–J)** Effect of CD44 knockdown on the migration and invasion capacity **(G, H)** and FAO **(I, J)** of HGC-27 and HGC-27-L; **(K)** CD44 protein detection in exosomes derived from HGC-27 and HGC-27-L with CD44 knockdown; **(L–O)** Effect of CD44-less exosomes on migration and invasion capacity **(L, M)** and FAO **(N, O)** of AGS; **(P–R)** Effect of CD44-less exosomes on LNM capacity of AGS in vivo. Ruler unit, mm. CHX, cycloheximide; ex, exosomes. *$P < 0.05$; **$P < 0.01$; ***$P < 0.001$.